Modeling Doxorubicin Delivery in Tumor Cells

Introduction

Doxorubicin Function and Side Effects

Doxorubicin is a commonly used drug in chemotherapy because it has a cytotoxic effect on dividing cells [1]. The molecule binds with topoisomerase II, which is a protein involved in the unwinding of DNA during cell division [2]. This function makes doxorubicin an effective drug to kill cancer cells, but it is also toxic to healthy dividing cells [2]. This cytotoxicity leads to negative side effects, such as hair loss, stomach ulcers, and other symptoms indicative of cell death of rapidly dividing cells [2]. Additionally, doxorubicin has been linked to increases in reactive oxygen species (ROS) [3]. This is of particular concern because ROS can cause oxidative stress in cells, to which the heart is particularly vulnerable [3]. Figure 1 summarizes the cytotoxic mechanisms of DOX. It is therefore vital that doxorubicin is delivered in a targeted way such that it can effectively kill the cancer cells while limiting the concentration in the rest of the body.

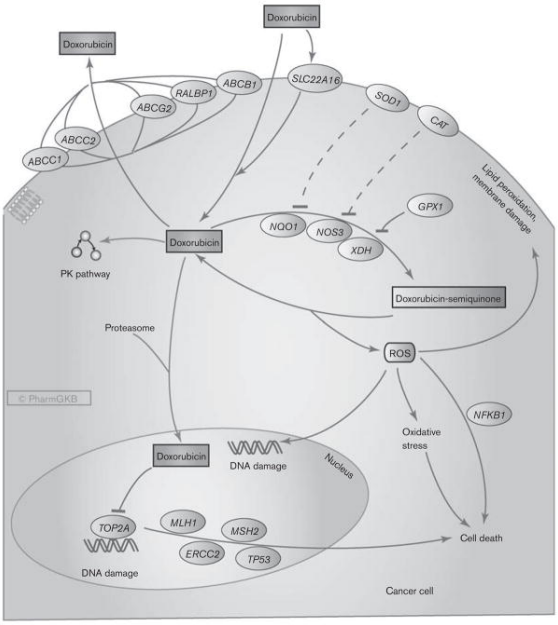

Figure 1: Mechanism of Action of Doxorubicin in a Cancer Cell. Doxorubicin targets the cells by preventing DNA transcription and the production of reactive oxygen species. *Image from Thorn et al.*

Drug Delivery Methods

Doxorubicin is typically delivered through the bloodstream, as either a bolus injection or a continuous perfusion via IV [4]. These methods create a baseline circulating concentration of the drug, which will be passively transported from the blood vessels, to the extracellular space, to inside cells. These methods generate a circulating concentration of the drug throughout the body, so healthy dividing cells will be equally exposed to the drug as tumor cells. Furthermore, the doxorubicin will be cycling through the heart, which can be dangerous due to the ROS

increase associated with doxorubicin. Therefore, the amount of drug that can be administered is limited by these negative side effects.

Targeted drug delivery is an approach that may circumvent the trade-off between high drug dose and increased risk from side-effects [4]. One such approach is the encapsulation of free drug in liposomes. These liposomes can then be delivered to the bloodstream, where they will slowly degrade, which will decrease the concentration of circulating doxorubicin. Additionally, these liposomes can be created in such a way that makes them sensitive to heat. This allows clinicians to create targeted regions of high drug concentration based on where heat is applied.

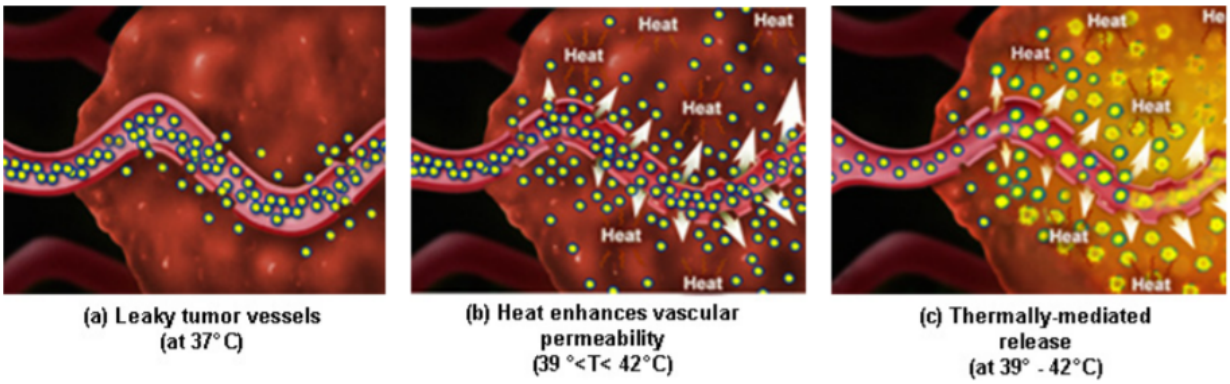

Figure 2: Process of Liposomal Drug Delivery. a) Liposomes circulating in bloodstream and passively transport out of the vasculature into the extracellular space. b) Added heat increases the permeability of the blood vessels, resulting in higher concentrations of liposomes in the extracellular space. c) Heat causes the liposomes to dissociate and release the drug into the extracellular space, where it can be transported into cells. *Image from Landon et al.*

Methods:

In this project, we implemented the equations published by El-Kareh and Secomb [5] to model the delivery of doxorubicin through a bolus injection and liposomal delivery. The liposomal delivery was also modeled in 2 different methods: free release and thermally sensitive release. In order to find a numerical solution, a 4th order Runge Kutta method was used to approximate a solution. The terms of the Runge Kutta method can be described as follows:

$$k_0 = \frac{dy}{dt}(y(t_0), t_0)$$
$$k_1 = \frac{dy}{dt}(y(t_0 + \frac{k_0 \Delta t}{2}), t_0 + \frac{\Delta t}{2})$$
$$k_2 = \frac{dy}{dt}(y(t_0 + \frac{k_1 \Delta t}{2}), t_0 + \frac{\Delta t}{2})$$
$$k_3 = \frac{dy}{dt}(y(t_0 + k_2 \Delta t), t_0 + \frac{\Delta t}{2})$$

The same equations were used to model the concentrations of each of the different compartments. For the bolus injection of free drug, the concentration of doxorubicin is described

in the vessels, extracellular space, and intercellular space. These concentrations are characterized as follows:

$$c_v(t) = DAe^{-\alpha t}$$

$$\frac{dc_i}{dt} = V_{max}\left(\frac{c_e}{c_{e+K_e\phi}} - \frac{c_i i}{c_i + k_i}\right)$$

$$\frac{dc_e}{dt} = PS_t(c_v - c_e) - d_c V_{max}\left(\frac{c_e}{c_e + K_e\phi} - \frac{c_i i}{c_i + k_i}\right)$$

The liposomal delivery is modelled as follows:

$$\frac{dc_i}{dt} = V_{max}\left(\frac{c_e}{c_{e+K_e\phi}} - \frac{c_i i}{c_i + k_i}\right)$$

$$\frac{dc_e}{dt} = PS_t(c_v - c_e) - d_c V_{max}\left(\frac{c_e}{c_e + K_e\phi} - \frac{c_i i}{c_i + k_i}\right) + \frac{c_{le}}{\tau_{re}}$$

$$c_{Lv}(t) = \frac{D}{D_G}\left(A_1 e^{-k_1 t} + A_2 e^{-k_2 t}\right)$$

$$\frac{dc_{Le}}{dt} = P_L S_t(c_{Lv} - c_{Le}) - \frac{c_{Le}}{\tau_{re}}$$

$$\frac{dc_v}{dt} = -\frac{V_t}{V_B} PS_t(c_v - c_e) + AV_B \frac{c_{Lv}}{\tau_{rv}} - (\alpha * c_v)$$

We modeled the release of free drug from the thermally activated liposomes as a change in the time constant (τ_{re}).

$$\tau^0{}_{re}\ if\ t < t_h\ or\ t > t_h + t_d$$

$$\tau^h{}_{re}\ if\ t_h < t < t_h + t_d$$

The time constants follow a step function where the rate of release is constant until the input time is reached. At the time of this signal, the time constant is increased so that drug is released faster. The time constant then returns to the baseline value after a specified amount of time. The constants used are taken from the table found in [5] as shown below.

Symbol	Description	Value
MW	molecular weight of doxorubicin	544
L	typical spacing between microvessels in tumor	200 μm
D_t	diffusivity of doxorubicin in tumor	1.6×10^{-6} cm/s^2
D	total dose of doxorubicin injected	100–285 mg (free), 20–350 mg (liposomal)
S_t	vascular (surface) density in tumor	200 cm^{-1}
P	tumor vascular permeability for doxorubicin	1.0×10^{-4} cm/s
V_B	total blood volume in body	5.0 l
V_t	total tumor volume	50 ml
d_c	cell density	6×10^8 cells/ml
ϕ	volume fraction of extracellular space (tumor)	0.4
$t^{\alpha}_{1/2}$	initial plasma half-life of doxorubicin	4.75 min
α	time constant for doxorubicin in plasma	$0.693/t^{\alpha}_{1/2}$
A	inverse volume of distribution in plasma	0.13/l
V_{max}	rate constant in kinetics for cellular transmembrane transport	0.28 ng/(10^5 cells)/min
K_e	Michaelis constant for cellular transmembrane transport	0.219 μg/ml
K_l	Michaelis constant for cellular transmembrane transport	1.37 ng/(10^5 cells)
P_L, P^0_L	tumor vascular permeability of liposomes	3.4×10^{-7} cm/s
t_d	duration of hyperthermia	60 min
t_h	time after injection when hyperthermia starts	120 min
E	enhancement factor for P_L at 45°C	1–100
A_1	plasma pharmacokinetic parameter for liposomes	6.9 μg/ml
A_2	plasma pharmacokinetic parameter for liposomes	12.2 μg/ml
k_1	plasma pharmacokinetic parameter for liposomes	0.00502 min^{-1}
k_2	plasma pharmacokinetic parameter for liposomes	0.00025 min^{-1}
D_G	dose corresponding to A_1, A_2, k_1, k_2	50 mg/m^2
τ_{re}, τ^0_{re}	time constant for liposome rupture in tumor extracellular space	24 h
τ^h_{re}	time constant for liposome rupture in tumor extracellular space at 45°C	0.72 min
τ_{rv}, τ^0_{rv}	time constant for liposome rupture in plasma	24 h
τ^h_{rv}	time constant for liposome rupture in plasma at 45°C	0.72 min

Finally, as an extension to the work of El-Kareh and Secomb, we model a pulsed injection of heat. Rather than releasing applying heat for a single interval t_h to $t_h + t_d$, we instead apply heat for the intervals described by $t_h + n\Delta T$to $t_h + n\Delta T + t_d$. Parameters used for this portion of the simulation are found in the following table.

t_h	120 ms
t_d	10 ms
n	0,1,2,3,4,5
ΔT	120 ms

Results:

The aforementioned equations were manually implemented in MATLAB. Scripts used for the numerical implementation are located in the appendix.

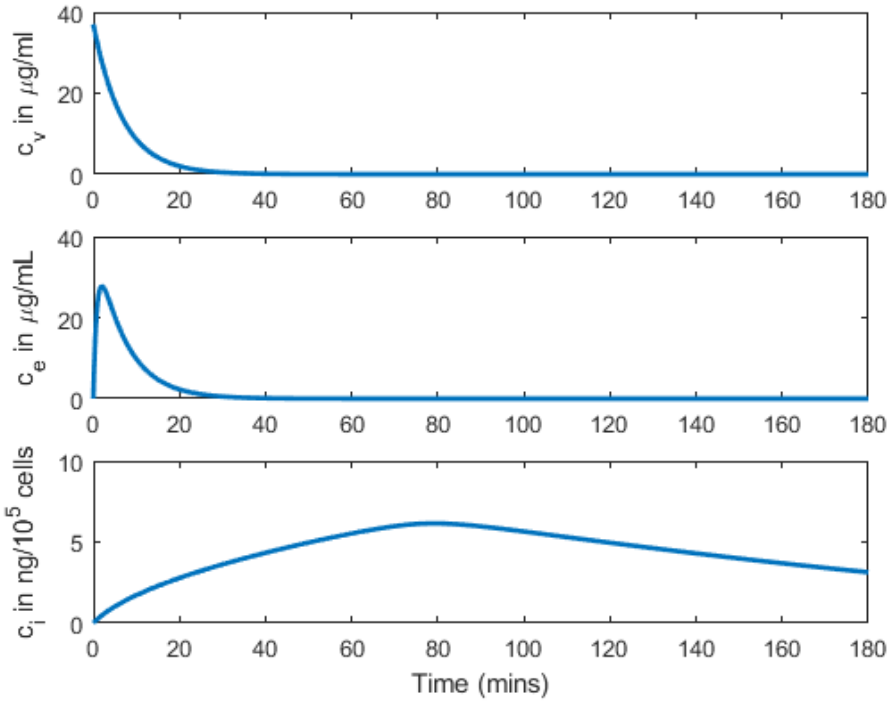

Fig 3: The solution to the bolus injection implementation

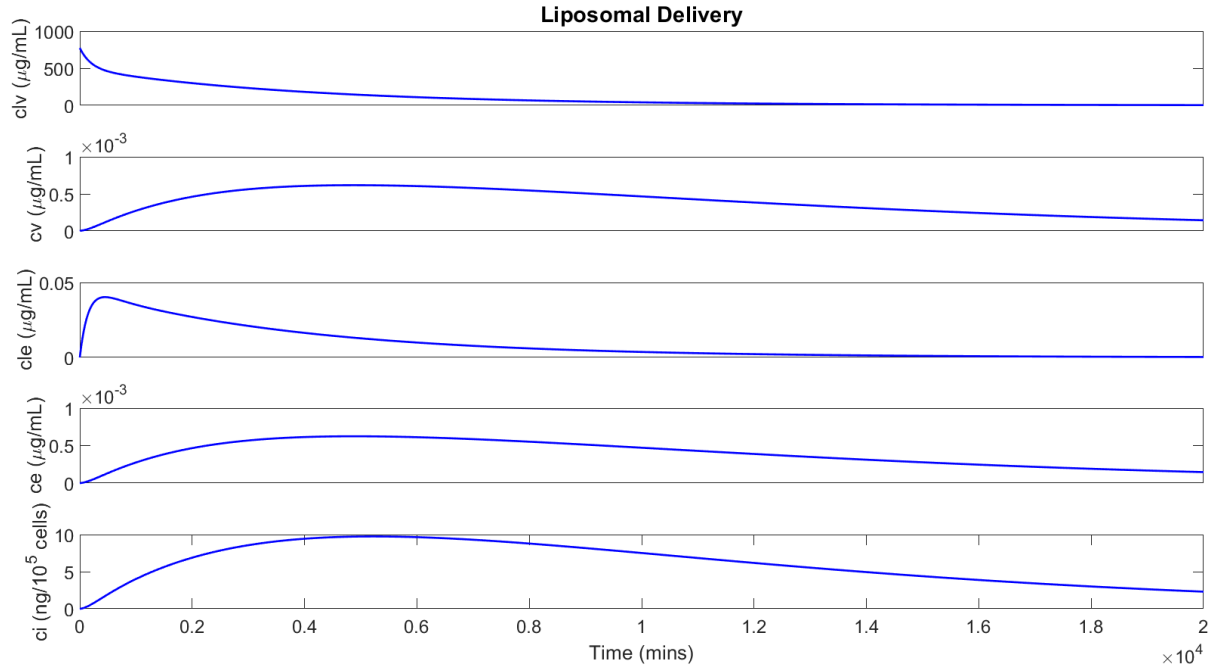

Fig 4: The solutions to the liposomal delivery implementation

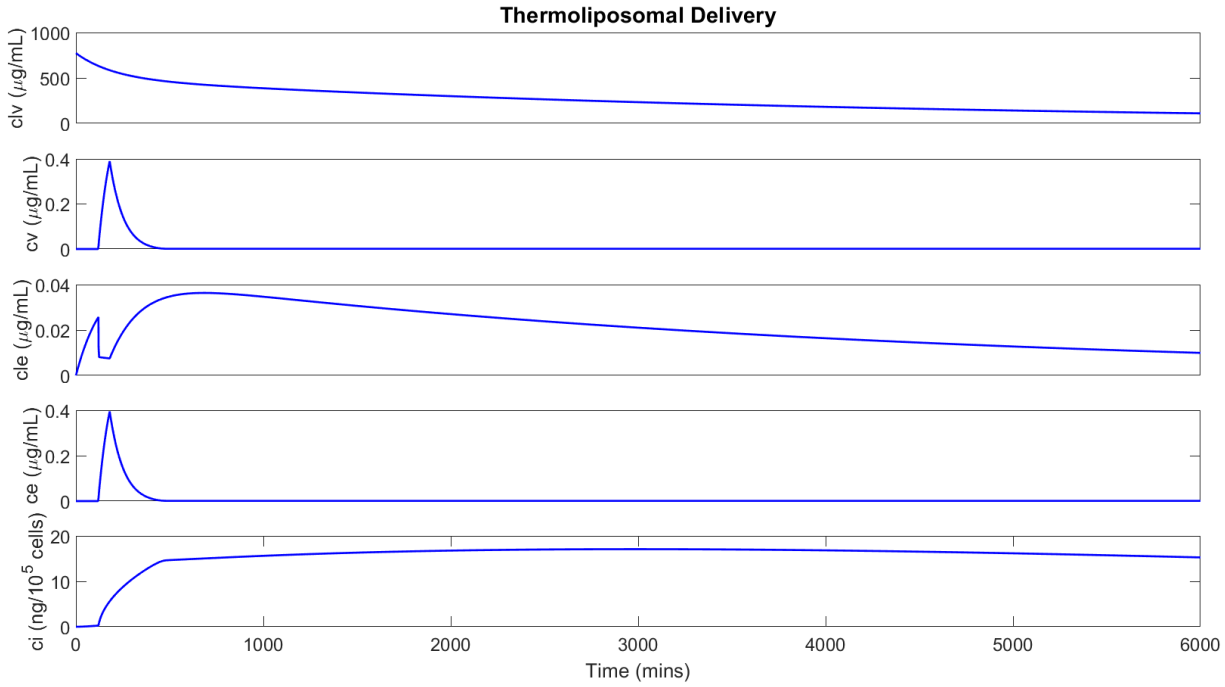

Fig 5: The solutions to the thermally activated liposomal delivery

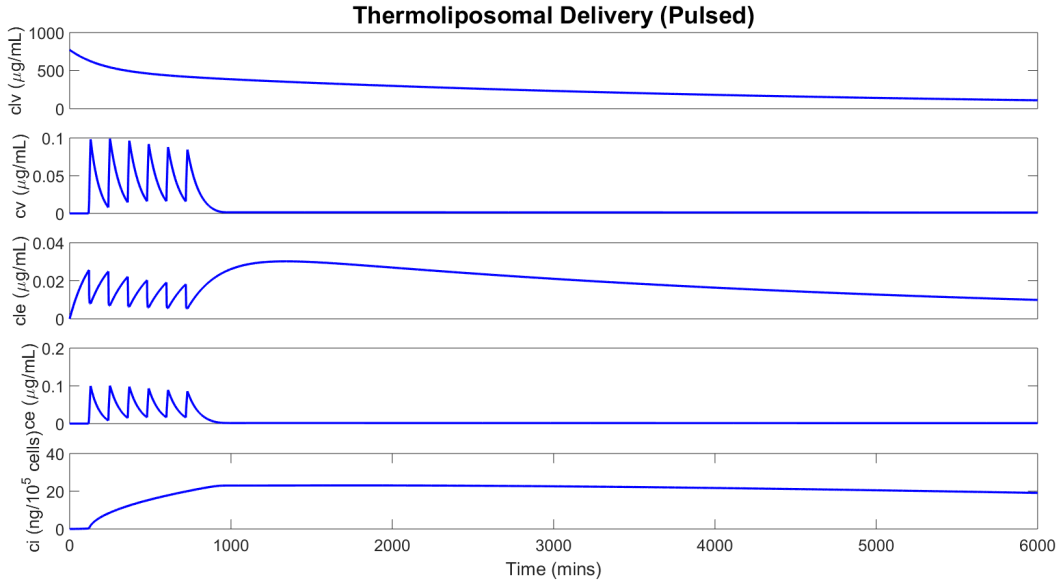

Fig 6: The solutions to the pulsed thermally activated liposomal delivery

Liposomal injection reduces free drug in bloodstream

One of the primary goals of targeted drug delivery it to reduce the concentration of free drug in the bloodstream. As seen in Figure 1, concentration of free drug in the bloodstream following bolus injection reached nearly 40 ug/mL. This value was much greater than the ~13 ug/mL modeled by El-Kareh and Secomb, but our model still showed a quick decrease to 0, showing

that the larger concentration would still quickly diffuse into the cells. Following non-thermally activated liposomal drug delivery, the concentration reached a maximum of 0.0006 ug/mL. Following thermally activated drug delivery, the concentration reached a maximum of 0.4 ug/mL, a 100-fold improvement over the free drug bolus injection. These concentrations are much less than the published values of ~12 and ~8 ug/mL, showing that our model may show better diffusion under these conditions.

Thermally activated liposomal injection increases concentration of free drug in tumor

In implementing targeted drug delivery, it is also important to devise a system in which the concentration of free drug in the tumor does not drop significantly below the level observed following bolus injection. Concentration of free drug in the tumor reached a maximum of 5.5 ng/10^5 cells following bolus injection. This agrees with the published concentration found by El-Kareh and Secomb. Following non-thermally activated liposomal drug delivery, the concentration reached a maximum of 10 ng/10^5 cells, albeit at a much longer time scale. This is very similar to the published value of 6 ng/10^5 cells. Following thermally activated drug delivery, the concentration reached a maximum of nearly 20 ng/10^5 cells. This is a much larger concentration than the 5 ng/10^5 cells shown in the literature, showing that our model may be less optimal for the thermally activated liposomes.

Short pulses of heat provide better performance than single, longer-term activation

Using pulse heat injection reduced the maximum concentration of free drug in the bloodstream by a factor of 4 in comparison with the original thermal activation model. Furthermore, this scheme resulted in a higher concentration of free drug at the tumor. At t = 3000 minutes, far after both heating schemes were finished, concentration of free drug at the tumor was 32% higher for the pulsed injection method.

Discussion

The fundamental goal of liposomal drug delivery is to reduce the concentration of free drug in the bloodstream, while increasing the concentration of free drug in the tumor. The model implemented indicates that this is a worthwhile area of pursuit to achieve these goals. By achieving this, clinicians will be able to reduce the side-effects of chemotherapy by localizing the delivery to the tumor region. By generating an easily updated mathematical model, we can also provide a tool that allows clinicians to test a personalized therapeutic approach before treatment starts. We improved the model by El-Kareh and Secomb by showing increased performance as a result of pulsed activation of thermoliposomes in comparison to a single, longer activation. Further models should be developed which better account for the spatial geometry of human tissue, which will better predict the localized release of doxorubicin, especially in highly-vascularized regions.

Our model showed the effects of targeted doxorubicin release generally in the vasculature, but it could additionally be targeted to specific tissue interfaces such as the blood brain barrier, or for

specific maladies such as non-Hodgkin's lymphoma. This could be done by combining our model with previously published models that include these specifications [6-7]. Additionally as in the work done by Ribba et al [7], this model can be used to both determine the optimal concentration and heating needed for the individual patient and can determine the efficacy of standard protocols.

References:

[1] Lal, S., Mahajan, A., Ning Chen, W., & Chowbay, B. "Pharmacogenetics of target genes across doxorubicin disposition pathway: a review." *Current drug metabolism*, vol.11, no.1, pp. 115-128, 2010.

[2] Thorn, C. F., Oshiro, C., Marsh, S., Hernandez-Boussard, T., McLeod, H., Klein, T. E., & Altman, R. B. "Doxorubicin pathways: pharmacodynamics and adverse effects." *Pharmacogenetics and genomics*, vol. 21, no. 7, pp. 440, 2011.

[3] Carvalho, C., Santos, R. X., Cardoso, S., Correia, S., Oliveira, P. J., Santos, M. S., & Moreira, P. I. "Doxorubicin: the good, the bad and the ugly effect." *Current medicinal chemistry*, vol. 15, no. 25, pp. 3267-3285, 2009.

[4] Landon, C. D., Park, J. Y., Needham, D., & Dewhirst, M. W. "Nanoscale drug delivery and hyperthermia: the materials design and preclinical and clinical testing of low temperature-sensitive liposomes used in combination with mild hyperthermia in the treatment of local cancer." *The Open Nanomedicine Journal*, vol. 3, no. 38, 2001.

[5] A. El-Kareh and T. Secomb, "A Mathematical Model for Comparison of Bolus Injection, Continuous Infusion, and Liposomal Delivery of Doxorubicin to Tumor Cells." *Neoplasts,* vol 2, no. 4, pp 325-338, 2000.

[6] Nhan, T., Burgess, A., Lilge L, Hynynen K. "Modeling Localized Delivery of Doxorubicin to the brain following focused ultrasound enhanced blood-brain barrer permeability." *Physics in Medicine and Biology*, vol. 59, no. 20, 2014.

[7] Ribba, B., Marron, K., Agur, Z., Alarcon, T., Maini, P.K. "A mathematical model of Doxorubicin treatment efficacy for non-Hodgkin's lymphoma: investigation of the current protocol through theoretical modelling results." *Bulletin of Mathematical Biology*, vol. 67, pp 79-99, 2005.

Appendix A: MATLAB Code

```
clear; clc; close all

%% Bolus Injection

% Parameters
h = 0.01;
tfinal = 180;
Vmax = .28*1e-6; %mg/10^5cells/min
P = 1e-4*60; %cm/min
St = 200; %cm^-1
D = 285; %mg (free)
A = .13; %(1/L)
t_half = 4.75; %min
```

```
alpha = .693/t_half;
dc = 6e3; %10^5cells/mL
ke = .219/1e3; %mg/mL
ki = 1.37; %ng/(10^5 cells)
phi = .4;

% Initial Condition
t(1) = 0;
ce(1) = 0;
ci(1) = 0;

% Define the ODE function handles
% First for bolus injection
cv = @(x) D*A*exp(-alpha*x);
dcedt = @(x,ce,ci) P*St*(cv(x)-ce)-dc*Vmax*((ce/(ce+(ke*phi))-(ci/(ci+ki))));
dcidt = @(x,ce,ci) 1e6*Vmax*((ce/(ce+(ke*phi)))-(ci/(ci+ki))); % 1e6 correction from mg to
ng

for i = 1:ceil(tfinal/h)
    t(i+1) = t(i)+h;

    % First order Terms
    k0=h*dcedt(t(i),ce(i),ci(i));
    l0=h*dcidt(t(i),ce(i),ci(i));

    % Second order terms
    k1=h*dcedt(t(i)+h/2,ce(i)+k0/2,ci(i)+l0/2);
    l1=h*dcidt(t(i)+h/2,ce(i)+k0/2,ci(i)+l0/2);

    % Third order terms
    k2=h*dcedt(t(i)+h/2,ce(i)+k1/2,ci(i)+l1/2);
    l2=h*dcidt(t(i)+h/2,ce(i)+k1/2,ci(i)+l1/2);

    % Fourth order terms
    k3=h*dcedt(t(i)+h,ce(i)+k2,ci(i)+l2);
    l3=h*dcidt(t(i)+h,ce(i)+k2,ci(i)+l2);

    ce(i+1) = ce(i) + (1/6)*(k0+2*k1+2*k2+k3);
    ci(i+1) = ci(i) + (1/6)*(l0+2*l1+2*l2+l3);
end

figure;
subplot(3,1,1);plot(t,cv(t));ylabel('c_v');
subplot(3,1,2);plot(t,ce);ylabel('c_e');
subplot(3,1,3);plot(t,ci);ylabel('c_i');

%% Next for Liposomal Injection

clear t
% Parameters
D_L = 350; %mg
DG = 86.5; % mg
A1 = 6.9/1e3; % mg/ml
A2 = 12.2/1e3; % mg/ml
Kk1 = 0.00502; % 1/min
Kk2 = 0.00025; % 1/min
PL = 3.4e-7*60; %cm/min
ST = 200; %1/cm
taure = 24*60; % minutes
taurv = 24*60; % minutes
```

```
Vt = 50; %mL
VB = 5; %L

tfinal = 20000; % Larger time scale needed for slow release liposomes
h = 0.1;

% Define the ODE function handles
% New equations
clv = @ (x) (D_L/DG)*(A1*exp(-Kk1*x)+A2*exp(-Kk2*x));
dcv_lipdt = @ (x,cv_lip,cle,ce_lip) (-Vt/VB)*P*ST*(cv_lip-ce_lip)+A*VB*(clv(x)/taurv)-
alpha*cv_lip;
dcledt = @ (x,cle) PL*St*(clv(x)-cle)-(cle/taure);
% Include a term in the equation below to represent release from liposomes
dce_lipdt = @(x,ce_lip,ci_lip,cle,cv_lip) P*St*(cv_lip-ce_lip)-
dc*Vmax*((ce_lip/(ce_lip+(ke*phi))-(ci_lip/(ci_lip+ki))))+cle/taure;
% No change in the equation below
dci_lipdt = @(x,ce_lip,ci_lip) 1e6*Vmax*((ce_lip/(ce_lip+(ke*phi)))-(ci_lip/(ci_lip+ki)));

% Initial Condition
t(1) = 0;
cv_lip(1) = 0;    %mg/mL
cle(1) = 0;
ce_lip(1) = 0;
ci_lip(1) = 0;

% Use Runge-Kutta to Solve for cv, cle, ce, ci
for i = 1:ceil(tfinal/h)
    t(i+1) = t(i)+h;

    % First order Terms
    k0=h*dcv_lipdt(t(i),cv_lip(i),cle(i),ce_lip(i));                                % K
terms = dcvdt
    l0=h*dcledt(t(i),cle(i));                                                       % L
terms = dcledt
    m0=h*dce_lipdt(t(i),ce_lip(i),ci_lip(i),cle(i),cv_lip(i));                      % M
terms = dcedt
    n0=h*dci_lipdt(t(i),ce_lip(i),ci_lip(i));                                       % N
terms = dcidt

    % Second order terms
    k1=h*dcv_lipdt(t(i)+h/2,cv_lip(i)+k0/2,cle(i)+l0/2,ce_lip(i)+m0/2);
    l1=h*dcledt(t(i)+h/2,cle(i)+l0/2);
    m1=h*dce_lipdt(t(i),ce_lip(i)+m0/2,ci_lip(i)+n0/2,cle(i)+l0/2,cv_lip(i)+k0/2);
    n1=h*dci_lipdt(t(i),ce_lip(i)+m0/2,ci_lip(i)+n0/2);

    % Third order terms
    k2=h*dcv_lipdt(t(i)+h/2,cv_lip(i)+k1/2,cle(i)+l1/2,ce_lip(i)+m1/2);
    l2=h*dcledt(t(i)+h/2,cle(i)+l1/2);
    m2=h*dce_lipdt(t(i),ce_lip(i)+m1/2,ci_lip(i)+n1/2,cle(i)+l1/2,cv_lip(i)+k1/2);
    n2=h*dci_lipdt(t(i),ce_lip(i)+m1/2,ci_lip(i)+n1/2);

    % Fourth order terms
    k3=h*dcv_lipdt(t(i)+h,cv_lip(i)+k2,cle(i)+l2,ce_lip(i)+m2);
    l3=h*dcledt(t(i)+h,cle(i)+l2);
    m3=h*dce_lipdt(t(i)+h,ce_lip(i)+m2,ci_lip(i)+n2,cle(i)+l2,cv_lip(i)+k2);
    n3=h*dci_lipdt(t(i)+h,ce_lip(i)+m2,ci_lip(i)+n2);

    cv_lip(i+1) = cv_lip(i) + (1/6)*(k0+2*k1+2*k2+k3);
    cle(i+1) = cle(i) + (1/6)*(l0+2*l1+2*l2+l3);
    ce_lip(i+1) = ce_lip(i) + (1/6)*(m0+2*m1+2*m2+m3);
```

```
    ci_lip(i+1) = ci_lip(i) + (1/6)*(n0+2*n1+2*n2+n3);
end

clear k0 k1 k2 k3 l0 l1 l2 l3 m0 m1 m2 m3 n0 n1 n2 n3

figure;
subplot(5,1,1);plot(t,clv(t));ylabel('clv');
subplot(5,1,2);plot(t,cv_lip);ylabel('cv');
subplot(5,1,3);plot(t,cle);ylabel('cle');
subplot(5,1,4);plot(t,ce_lip);ylabel('ce');
subplot(5,1,5);plot(t,ci_lip);ylabel('ci');


%% Next for thermoliposome injection
clear t

% Parameters
td = 60; % Duration of hyperthermia (min)
th  = 120; % Time after injection hyperthermia starts (min)
taurelow = 24*60; % minutes
taurvlow = 24*60; % minutes
taurehigh = 0.72; % (min)
taurvhigh = 0.72; % (min)
E = 50; % Enhancement factor on tumor permeability of liposomes

tfinal = 6000; % Larger time scale needed for slow release liposomes
h = 0.1;

% Define the ODE function handles
% No new ODE equations

% Initial Condition
t(1) = 0;
Tcv_lip(1) = 0;    %mg/mL
Tcle(1) = 0;
Tce_lip(1) = 0;
Tci_lip(1) = 0;

% Redefine the ODE function handles
% New equations
clv = @ (x) (D_L/DG)*(A1*exp(-Kk1*x)+A2*exp(-Kk2*x));
dcv_lipdt = @ (x,cv_lip,cle,ce_lip) (-Vt/VB)*P*ST*(cv_lip-ce_lip)+A*VB*(clv(x)/taurv)-
alpha*cv_lip;
dcledt = @ (x,cle) PL*St*(clv(x)-cle)-(cle/taure);
% Include a term in the equation below to represent release from liposomes
dce_lipdt = @(x,ce_lip,ci_lip,cle,cv_lip) P*St*(cv_lip-ce_lip)-
dc*Vmax*((ce_lip/(ce_lip+(ke*phi))-(ci_lip/(ci_lip+ki))))+cle/taure;
% No change in the equation below
dci_lipdt = @(x,ce_lip,ci_lip) 1e6*Vmax*((ce_lip/(ce_lip+(ke*phi)))-(ci_lip/(ci_lip+ki)));

% Use Runge-Kutta to Solve for cv, cle, ce, ci
for i = 1:ceil(tfinal/h)
    t(i+1) = t(i)+h;

    % First order Terms
    k0=h*dcv_lipdt(t(i),Tcv_lip(i),Tcle(i),Tce_lip(i));                                  % K
terms = dcvdt
    l0=h*dcledt(t(i),Tcle(i));                                                          % L
terms = dcledt
    m0=h*dce_lipdt(t(i),Tce_lip(i),Tci_lip(i),Tcle(i),Tcv_lip(i));                       % M
```

```
terms = dcedt
    n0=h*dci_lipdt(t(i),Tce_lip(i),Tci_lip(i));                                          % N
terms = dcidt

    % Second order terms
    k1=h*dcv_lipdt(t(i)+h/2,Tcv_lip(i)+k0/2,Tcle(i)+l0/2,Tce_lip(i)+m0/2);
    l1=h*dcledt(t(i)+h/2,Tcle(i)+l0/2);
    m1=h*dce_lipdt(t(i),Tce_lip(i)+m0/2,Tci_lip(i)+n0/2,Tcle(i)+l0/2,Tcv_lip(i)+k0/2);
    n1=h*dci_lipdt(t(i),Tce_lip(i)+m0/2,Tci_lip(i)+n0/2);

    % Third order terms
    k2=h*dcv_lipdt(t(i)+h/2,Tcv_lip(i)+k1/2,Tcle(i)+l1/2,Tce_lip(i)+m1/2);
    l2=h*dcledt(t(i)+h/2,Tcle(i)+l1/2);
    m2=h*dce_lipdt(t(i),Tce_lip(i)+m1/2,Tci_lip(i)+n1/2,Tcle(i)+l1/2,Tcv_lip(i)+k1/2);
    n2=h*dci_lipdt(t(i),Tce_lip(i)+m1/2,Tci_lip(i)+n1/2);

    % Fourth order terms
    k3=h*dcv_lipdt(t(i)+h,Tcv_lip(i)+k2,Tcle(i)+l2,Tce_lip(i)+m2);
    l3=h*dcledt(t(i)+h,Tcle(i)+l2);
    m3=h*dce_lipdt(t(i)+h,Tce_lip(i)+m2,Tci_lip(i)+n2,Tcle(i)+l2,Tcv_lip(i)+k2);
    n3=h*dci_lipdt(t(i)+h,Tce_lip(i)+m2,Tci_lip(i)+n2);

    Tcv_lip(i+1) = Tcv_lip(i) + (1/6)*(k0+2*k1+2*k2+k3);
    Tcle(i+1) = Tcle(i) + (1/6)*(l0+2*l1+2*l2+l3);
    Tce_lip(i+1) = Tce_lip(i) + (1/6)*(m0+2*m1+2*m2+m3);
    Tci_lip(i+1) = Tci_lip(i) + (1/6)*(n0+2*n1+2*n2+n3);

    if abs(t(i)-th)<(h/2); % At the time where heat is first applied
        taure = taurehigh;
        PL = E * PL;

        clv = @ (x) (D_L/DG)*(A1*exp(-Kk1*x)+A2*exp(-Kk2*x));
        dcv_lipdt = @ (x,cv_lip,cle,ce_lip) (-Vt/VB)*P*ST*(cv_lip-
ce_lip)+A*VB*(clv(x)/taurv)-alpha*cv_lip;
        dcledt = @ (x,cle) PL*St*(clv(x)-cle)-(cle/taure);
        dce_lipdt = @(x,ce_lip,ci_lip,cle,cv_lip) P*St*(cv_lip-ce_lip)-
dc*Vmax*((ce_lip/(ce_lip+(ke*phi))-(ci_lip/(ci_lip+ki))))+cle/taure;
        dci_lipdt = @(x,ce_lip,ci_lip) 1e6*Vmax*((ce_lip/(ce_lip+(ke*phi)))-
(ci_lip/(ci_lip+ki)));

    elseif abs(t(i)-(th+td))<(h/2); % At the time where heat is removed
        taure = taurelow;
        PL = PL / E;

        clv = @ (x) (D_L/DG)*(A1*exp(-Kk1*x)+A2*exp(-Kk2*x));
        dcv_lipdt = @ (x,cv_lip,cle,ce_lip) (-Vt/VB)*P*ST*(cv_lip-
ce_lip)+A*VB*(clv(x)/taurv)-alpha*cv_lip;
        dcledt = @ (x,cle) PL*St*(clv(x)-cle)-(cle/taure);
        dce_lipdt = @(x,ce_lip,ci_lip,cle,cv_lip) P*St*(cv_lip-ce_lip)-
dc*Vmax*((ce_lip/(ce_lip+(ke*phi))-(ci_lip/(ci_lip+ki))))+cle/taure;
        dci_lipdt = @(x,ce_lip,ci_lip) 1e6*Vmax*((ce_lip/(ce_lip+(ke*phi)))-
(ci_lip/(ci_lip+ki)));
    end
end

clear k0 k1 k2 k3 l0 l1 l2 l3 m0 m1 m2 m3 n0 n1 n2 n3

figure;
subplot(5,1,1);plot(t,clv(t));ylabel('clv');
subplot(5,1,2);plot(t,Tcv_lip);ylabel('cv');
```

```
subplot(5,1,3);plot(t,Tcle);ylabel('cle');
subplot(5,1,4);plot(t,Tce_lip);ylabel('ce');
subplot(5,1,5);plot(t,Tci_lip);ylabel('ci');



%% Next for thermoliposome injection
clear t

% Parameters
td = 10; % Duration of hyperthermia (min)
ths  = [120,240,360,480,600,720]; % Time after injection hyperthermia starts (min)
taurelow = 24*60; % minutes
taurvlow = 24*60; % minutes
taurehigh = 0.72; % (min)
taurvhigh = 0.72; % (min)
E = 50; % Enhancement factor on tumor permeability of liposomes

tfinal = 6000; % Larger time scale needed for slow release liposomes
h = 0.1;

% Define the ODE function handles
% No new ODE equations

% Initial Condition
t(1) = 0;
Tcv_lip(1) = 0;    %mg/mL
Tcle(1) = 0;
Tce_lip(1) = 0;
Tci_lip(1) = 0;

% Redefine the ODE function handles
% New equations
clv = @ (x) (D_L/DG)*(A1*exp(-Kk1*x)+A2*exp(-Kk2*x));
dcv_lipdt = @ (x,cv_lip,cle,ce_lip) (-Vt/VB)*P*ST*(cv_lip-ce_lip)+A*VB*(clv(x)/taurv)-
alpha*cv_lip;
dcledt = @ (x,cle) PL*St*(clv(x)-cle)-(cle/taure);
% Include a term in the equation below to represent release from liposomes
dce_lipdt = @(x,ce_lip,ci_lip,cle,cv_lip) P*St*(cv_lip-ce_lip)-
dc*Vmax*((ce_lip/(ce_lip+(ke*phi))-(ci_lip/(ci_lip+ki))))+cle/taure;
% No change in the equation below
dci_lipdt = @(x,ce_lip,ci_lip) 1e6*Vmax*((ce_lip/(ce_lip+(ke*phi)))-(ci_lip/(ci_lip+ki)));

% Use Runge-Kutta to Solve for cv, cle, ce, ci
for i = 1:ceil(tfinal/h)
    for j = 1:length(ths)
        t(i+1) = t(i)+h;

        % First order Terms
        k0=h*dcv_lipdt(t(i),Tcv_lip(i),Tcle(i),Tce_lip(i));                                  %
K terms = dcvdt
        l0=h*dcledt(t(i),Tcle(i));                                                          % L
terms = dcledt
        m0=h*dce_lipdt(t(i),Tce_lip(i),Tci_lip(i),Tcle(i),Tcv_lip(i));
% M terms = dcedt
        n0=h*dci_lipdt(t(i),Tce_lip(i),Tci_lip(i));                                          %
N terms = dcidt

        % Second order terms
```

```
        k1=h*dcv_lipdt(t(i)+h/2,Tcv_lip(i)+k0/2,Tcle(i)+l0/2,Tce_lip(i)+m0/2);
        l1=h*dcledt(t(i)+h/2,Tcle(i)+l0/2);
        m1=h*dce_lipdt(t(i),Tce_lip(i)+m0/2,Tci_lip(i)+n0/2,Tcle(i)+l0/2,Tcv_lip(i)+k0/2);
        n1=h*dci_lipdt(t(i),Tce_lip(i)+m0/2,Tci_lip(i)+n0/2);

        % Third order terms
        k2=h*dcv_lipdt(t(i)+h/2,Tcv_lip(i)+k1/2,Tcle(i)+l1/2,Tce_lip(i)+m1/2);
        l2=h*dcledt(t(i)+h/2,Tcle(i)+l1/2);
        m2=h*dce_lipdt(t(i),Tce_lip(i)+m1/2,Tci_lip(i)+n1/2,Tcle(i)+l1/2,Tcv_lip(i)+k1/2);
        n2=h*dci_lipdt(t(i),Tce_lip(i)+m1/2,Tci_lip(i)+n1/2);

        % Fourth order terms
        k3=h*dcv_lipdt(t(i)+h,Tcv_lip(i)+k2,Tcle(i)+l2,Tce_lip(i)+m2);
        l3=h*dcledt(t(i)+h,Tcle(i)+l2);
        m3=h*dce_lipdt(t(i)+h,Tce_lip(i)+m2,Tci_lip(i)+n2,Tcle(i)+l2,Tcv_lip(i)+k2);
        n3=h*dci_lipdt(t(i)+h,Tce_lip(i)+m2,Tci_lip(i)+n2);

        Tcv_lip(i+1) = Tcv_lip(i) + (1/6)*(k0+2*k1+2*k2+k3);
        Tcle(i+1) = Tcle(i) + (1/6)*(l0+2*l1+2*l2+l3);
        Tce_lip(i+1) = Tce_lip(i) + (1/6)*(m0+2*m1+2*m2+m3);
        Tci_lip(i+1) = Tci_lip(i) + (1/6)*(n0+2*n1+2*n2+n3);

        if abs(t(i)-ths(j))<(h/2); % At the time where heat is first applied
            taure = taurehigh;
            PL = E * PL;

            clv = @ (x) (D_L/DG)*(A1*exp(-Kk1*x)+A2*exp(-Kk2*x));
            dcv_lipdt = @ (x,cv_lip,cle,ce_lip) (-Vt/VB)*P*ST*(cv_lip-
ce_lip)+A*VB*(clv(x)/taurv)-alpha*cv_lip;
            dcledt = @ (x,cle) PL*St*(clv(x)-cle)-(cle/taure);
            dce_lipdt = @(x,ce_lip,ci_lip,cle,cv_lip) P*St*(cv_lip-ce_lip)-
dc*Vmax*((ce_lip/(ce_lip+(ke*phi))-(ci_lip/(ci_lip+ki))))+cle/taure;
            dci_lipdt = @(x,ce_lip,ci_lip) 1e6*Vmax*((ce_lip/(ce_lip+(ke*phi)))-
(ci_lip/(ci_lip+ki)));

        elseif abs(t(i)-(ths(j)+td))<(h/2); % At the time where heat is removed
            taure = taurelow;
            PL = PL / E;

            clv = @ (x) (D_L/DG)*(A1*exp(-Kk1*x)+A2*exp(-Kk2*x));
            dcv_lipdt = @ (x,cv_lip,cle,ce_lip) (-Vt/VB)*P*ST*(cv_lip-
ce_lip)+A*VB*(clv(x)/taurv)-alpha*cv_lip;
            dcledt = @ (x,cle) PL*St*(clv(x)-cle)-(cle/taure);
            dce_lipdt = @(x,ce_lip,ci_lip,cle,cv_lip) P*St*(cv_lip-ce_lip)-
dc*Vmax*((ce_lip/(ce_lip+(ke*phi))-(ci_lip/(ci_lip+ki))))+cle/taure;
            dci_lipdt = @(x,ce_lip,ci_lip) 1e6*Vmax*((ce_lip/(ce_lip+(ke*phi)))-
(ci_lip/(ci_lip+ki)));

            j = j+1;
        end
    end
end

clear k0 k1 k2 k3 l0 l1 l2 l3 m0 m1 m2 m3 n0 n1 n2 n3

figure;
subplot(5,1,1);plot(t,clv(t));ylabel('clv');
subplot(5,1,2);plot(t,Tcv_lip);ylabel('cv');
subplot(5,1,3);plot(t,Tcle);ylabel('cle');
subplot(5,1,4);plot(t,Tce_lip);ylabel('ce');
```

```
subplot(5,1,5);plot(t,Tci_lip);ylabel('ci');
```